INL/EXT-17-43117 Rev. 0

August 2017

Nuclear Energy Advanced Modeling and Simulation (NEAMS) Accident Tolerant Fuels High Impact Problem: U_3Si_2 Modeling Capabilities

K. A. Gamble
J. D. Hales
G. Pastore

INL/EXT-17-43117 Rev. 0

Nuclear Energy Advanced Modeling and Simulation (NEAMS) Accident Tolerant Fuels High Impact Problem: U_3Si_2 Modeling Capabilities

K. A. Gamble
J. D. Hales
G. Pastore

August 2017

Idaho National Laboratory
Fuel Modeling and Simulation Department
Idaho Falls, Idaho 83415

Prepared for the
U.S. Department of Energy
Office of Nuclear Energy
Under U.S. Department of Energy-Idaho Operations Office
Contract DE-AC07-05ID14517

Abstract

U_3Si_2 fuel is a potential candidate replacement for UO_2 in light water reactor fuel rods due to its higher uranium density and thermal conductivity. Its lower melting temperature and significant gaseous swelling may be of concern. The aggressive development schedule of the United States Department of Energy's (DOE) Advanced Fuels Campaign (AFC) to have potential accident tolerant fuels (ATF) concepts in lead test rods or assemblies as quickly as possible has necessitated the need for advanced modeling and simulation techniques to investigate the behavior of these materials under normal operating and accident conditions. This report presents the modeling capabilities for U_3Si_2 fuel at the engineering (continuum) scale developed as part of the Nuclear Energy Advanced Modeling and Simulation (NEAMS) high impact problem (HIP). In this report, the models incorporated into the BISON fuel for U_3Si_2 are described and comparisons to conventional UO_2 for separate effects cases are presented.

Contents

1 Introduction

The events that occurred at the Fukushima Daiichi Nuclear Power Plant in March 2011 were the precursor to increased research efforts into materials that provide enhanced tolerance under accident conditions. These materials were originally given the name accident tolerant fuels (ATF), and more recently advanced technology fuels to illustrate that current materials (UO_2 fuel and zirconium-based claddings) have some form of accident tolerance built into them. A candidate material is said to satisfy the requirements of enhanced accident tolerance if it provides significantly increased coping time in the event of an accident (e.g., Loss of Coolant Accident) while providing similar or improved performance as the conventional fuels rods used in current operation under normal operating conditions [1]. Qualitatively, ATF materials should have improved reaction kinetics with steam resulting in slower hydrogen generation rate and maintain acceptable thermo-mechanical behavior, fuel-to-clad interactions, and fission gas behavior. The Office of Nuclear Energy in the United States Department of Energy has for some time accelerated its research into potential ATF materials through the Advanced Fuels Campaign (AFC). The goal of this program was to guide selection of promising concepts for insertion into a commercial reactor as part of a lead test rod or assembly by 2022. Industry has recently accelerated that schedule.

The aggressive schedule for ATF material development prohibits the ability of performing a comprehensive set of experiments to provide the necessary data to draw conclusions on the accident tolerance of any given material. Therefore, computational analysis tools have been used to assist in the understanding of proposed ATF materials. This research has been performed through the Nuclear Energy Advanced Modeling and Simulation (NEAMS) high impact problem (HIP) program. Where possible a multiscale multiphysics approach has been used to develop mechanistic computer models for that have been incorporated into the engineering scale fuel performance code BISON [2–4]. One of the candidate materials being investigated by national laboratories, universities, and fuel vendors (Westinghouse) is U_3Si_2 fuel for its higher uranium density and thermal conductivity. A higher thermal conductivity is expected to reduce the radial temperature gradient within the fuel pellet resulting in less cracking and fission gas release. A higher uranium density provides the economic benefit of allowing utilities to use less fuel within the core for the same power produced. Some potential disadvantages of U_3Si_2 as a fuel material include its lower melting temperature ($\sim$1938 K) and large amounts of gaseous swelling.

In this report, we present the material model development for U_3Si_2 fuel and the application of these models under separate effects tests. Separate effects tests investigate the behavior of an

individual material model without influences from other models.

2 The Multiscale Approach

An issue associated with many of the proposed ATF materials is the lack of experimental data under power reactor operational conditions. The lack of experimental data prohibits the development of empirical correlations that describe the behavior of the fuel under these conditions. Therefore, a multiscale multiphysics approach is used that will provide mechanistic representations of the behavior under conditions for which experimental data is limited or non-existent. Lower length scale simulations including density functional theory (DFT), molecular dynamics (MD), phase field, and rate theory are used to understand the evolution of grain boundaries, defects (both interstitials and vacancies), dislocations, and fission gas bubbles and the influence they have on the thermo-mechanical and fission gas behavior of U_3Si_2 under reactor conditions. Typically the lowest length scale simulations (DFT and MD) are used to provide details of parameters that are used in the mesoscale (phase field and rate theory) calculations. The mesoscale models are then used to inform parameters that can be incorporated into a mechanistic equation to be added to BISON. A thermal conductivity model based upon phase field calculations has been incorporated into BISON in addition to a rate theory model for gaseous swelling and thermal conductivity degradation. The details of the lower length scale work completed as part of the NEAMS ATF HIP have been summarized previously in another report [5].

3 Material and Behavioral Models

The material and behavior models obtained from the existing literature or developed based upon lower length scale modeling and incorporated into BISON to facilitate fuel performance analyses of U_3Si_2 fuel include thermal and mechanical properties, swelling and fission gas behavior, and thermal and irradiation creep. The details of the models are described in this Chapter.

3.1 Thermal and Mechanical Properties

The thermal and mechanical properties of U_3Si_2 fuel include elastic properties, thermal conductivity, specific heat capacity, and thermal expansion.

3.1.1 Elastic Properties

The elastic properties of U_3Si_2 determines the mechanical response of the fuel under mechanical loading in the elastic regime. Limited experimental data exists regarding the temperature dependence of Young's modulus and Poisson's ratio, and the data that is available is based upon dispersion research reactor and not power reactor conditions. However, in the absence of other data, constant values of 140 GPa and 0.17 for Young's modulus and Poisson's ratio, respectively, are used as per Metzger et al. [6].

3.1.2 Thermal Conductivity

The thermal conductivity of U_3Si_2 is a measure of its ability conduct heat and appears in Fourier's Law for heat conduction. Three different models have been added to BISON to account for the evolution of thermal conductivity as a function of temperature, temperature gradient, and fission density (burnup).

3.1.2.1 Empirical

The empirical thermal conductivity model is a linear function of temperature based upon experiments by White et al. [7]:

$$k = 4.996 + 0.0118T \tag{3.1}$$

where k is the thermal conductivity in W/m-K and T is the temperature in K. This model is valid from 300 K to 1773 K.

3.1.2.2 Degradation

The thermal conductivity degradation model for U_3Si_2 uses the unirradiated thermal conductivity calculated by Equation 3.1 to calculate the intrinsic thermal conductivity. The intrinsic thermal conductivity is then multiplied by two degradation factors due to contributions from intergranular and intragranular bubbles. The model is based upon rate theory calculations [8] for which a tricubic interpolation algorithm was developed for incorporation into BISON. The model is a function of temperature, local temperature gradient, and fission density (burnup). The ranges of applicability of the model are temperatures from 390 K to 1190 K, temperature gradients from 0 to 160 K/mm and fission densities from 0 to 2.5755×10^{21} fissions/cm^3.

The intrinsic thermal conductivity is calculated as follows:

$$k_{in} = \frac{k_{white}}{1 - k_{white}\frac{R}{g}} \tag{3.2}$$

where k_{white} is thermal conductivity calculated by the White model, R is the Kapitza resistance (2.5e-8 m^2-K/W), and g is the grain size (taken as 35 μm).

The modified Kapitza resistance is determined based upon the amount of grain boundary coverage:

$$GB_{cov} = \frac{FCOV}{3000.0} \tag{3.3}$$

where GB_{cov} is the grain boundary coverage, and $FCOV$ is computed by the tricubic interpolation calculation. The modified Kapitza resistance is then determined by:

$$R' = R\left(1 - GB_{cov}\right)^{0.86+0.3ln(R)} \tag{3.4}$$

The intergranular factor is then computed by:

$$f_{inter} = \frac{1.0}{1.0 - k_{in}\frac{R'}{g_g}} \tag{3.5}$$

where g_g is the grain size specified in the GRASS-SST rate theory calculation. This value is taken as 5.0 μm. The intragranular factor is calculated by:

$$f_{intra} = \frac{1.0 - GSWb}{1.0 + 0.9GSWb} \tag{3.6}$$

where $GSWb$ is the intragranular gaseous swelling strain due to intragranular bubbles calculated by the tricubic interpolation calculation. Finally the thermal conductivity is then given as:

$$k = k_{in} f_{inter} f_{intra} \tag{3.7}$$

3.1.3 Specific Heat Capacity

The specific heat capacity of U_3Si_2 is measure of its ability to absorb heat per unit mass and is of particular importance during reactivity insertion accidents (RIA). The most recent model available in BISON is based upon the experiments of White et al. [7, 9]. In J/mol-K the specific heat is calculated via a linear function of temperature:

$$c_p = 140.5 + 0.02582T \tag{3.8}$$

The c_p value is then converted into units of J/kg-K by dividing by the molar mass of U_3Si_2 given by 0.770258 kg/mol.

3.1.4 Thermal Expansion

According to Metzger et al. [6] the linear thermal expansion coefficient is reported in multiple locations within the literature. The value chosen by those authors and used in this work is a constant value valid from 298 K to 1473 K of 15.0×10^{-6} K^{-1}.

3.2 Swelling and Fission Gas Behavior

The understanding of fission product swelling and fission gas release in U_3Si_2 is essential to predict the fuel performance of a fuel rod containing U_3Si_2 because it will directly influence the stress and strain states in both the fuel and cladding as well as the internal pressure of the rod. Three models have been developed for this purpose: empirical, rate theory, and coupled gas swelling and fission gas release. A densification model is also used that takes into account the sintering of the fuel early in life.

3.2.1 Densification

U_3Si_2 is expected to experience densification similar to UO_2 . Thus, the fuel densification is computed using the ESCORE empirical model [10] given by:

$$\varepsilon_D = \Delta\rho_0 \left(e^{\left(\frac{Bu\, ln(0.01)}{C_D Bu_D} \right)} - 1 \right) \tag{3.9}$$

where ε_D is the densification strain, $\Delta\rho_0$ is the total densification that can occur (given as a fraction of theoretical density), Bu is the burnup, and Bu_D is the burnup at which densification is complete. For temperatures below 750°C the parameter C_D is given by $7.2 - 0.0086(T - 25)$; above 750°C the parameter is 1.0 (T in °C).

3.2.2 Empirical Model

Since the data for U_3Si_2 is limited, an empirical expression for the swelling of U_3Si_2 was determined using data from Figure 3 of [11]. The swelling of fuel particles was calculated by Finlay using the results of miniplate irradiation tests. To convert Finlay's data (fission density) to FIMA, a value of 10.735 g/cm^3 was used as the heavy metal density, equivalent to 95% theoretical heavy metal density. Based on Finlay's data the volumetric strain can be written as a function of burnup:

$$\frac{dV}{V} = 3.8808 \times Bu^2 + 0.79811 \times Bu \tag{3.10}$$

where dV/V is the volumetric strain at a given burnup Bu. The burnup is in units of FIMA. The quadratic equation for the total volumetric strain is then decoupled into its solid and gaseous components. The solid swelling is a linear function of burnup based upon the data of Hofman [12] using the same conversion procedure from fission density to burnup given above:

$$\left(\frac{dV}{V}\right)_{solid} = 0.34392 \times Bu \tag{3.11}$$

which results in a gaseous swelling contribution given by the following quadratic function of burnup:

$$\left(\frac{dV}{V}\right)_{gaseous} = 3.8808 \times Bu^2 + 0.45419 \times Bu \tag{3.12}$$

3.2.3 Rate Theory Gaseous Swelling Model

The rate theory gaseous swelling model uses the same tricubic interpolation scheme as the thermal conductivity degradation model. In this case, the parameter called *GSW* representing the total gaseous swelling is calculated and used. The same ranges of applicability as the thermal conductivity degradation model apply to this model. The value calculated by this model is added to the solid swelling given by Equation 3.11 and the densification given by Equation 3.9 to determine the total volumetric change.

3.2.4 Combined Gaseous Swelling and Fission Gas Release

The combined gaseous swelling and fission gas release model handles fission gas swelling and release in U_3Si_2 under power reactor conditions. The model calculates the coupled fission gas swelling and release concurrently and is physically based. This model relies on the current understanding of microstructure and fission gas behavior in U_3Si_2, including the recent findings from lower-length scale modeling and the available experimental data. Based on the experimental evidence from [13], we assume U_3Si_2 remains crystalline at power reactor temperatures. We also assume both intra-granular and grain-boundary gas bubbles develop, as in UO_2.

In order to mitigate the scarcity of experimental data, new physically based descriptions of specific processes can be informed with U_3Si_2 material parameters which have been extracted from lower-length scale modeling. Furthermore, the physical interpretation of some relevant processes differ from the interpretation in the existing UO_2 model in BISON to better conform to the current understanding of fission gas behavior in U_3Si_2. These processes include:

1. Modeling of intra-granular bubble nucleation and re-solution based on the so-called homogeneous mechanisms

2. Modeling intra-granular bubble growth considering absorption of vacancies by the bubbles and based on an adaptation of the Speight-Beere model.

Material parameters are taken from lower-length scale calculations for U_3Si_2, where available. Parameters for which specific U_3Si_2 values are not yet available are given acceptable values based on data for metals, theoretical considerations or the best fitting of model results to experimental data. The model presented here is an initial engineering-scale fission gas model for U_3Si_2 that incorporates state-of-the-art understanding and lower-length scale modeling data and will be progressively updated as new data become available.

3.2.4.1 Intra-granular gas behavior

The model accounts for nucleation of bubbles, re-solution of gas from bubbles to the matrix, and trapping of gas from the matrix into the bubbles. Fission gas transport from within the fuel grains to the grain faces is computed by the numerical solution of the diffusion equation in one-dimensional spherical geometry.

Nucleation and re-solution may occur by different mechanisms, i.e., heterogeneous and homogeneous [14]. Heterogeneous nucleation and re-solution refer to the creation of new bubble nuclei as a direct consequence of the interaction of fission fragments with the lattice and bubble destruction occurring en bloc by passing fission fragments, respectively. The homogeneous mechanisms account for the nucleation of bubbles by diffusion-driven interactions of dissolved gas atoms and re-solution occurring gradually by ejection of individual atoms. The dominant mechanisms depend upon the nature of the interactions between fission fragments and lattice (electronic or phononic). Based on [15], we assume the homogeneous mechanisms to dominate in U_3Si_2. The equations for the evolution of the intra-granular gas bubble number density and gas atom concentrations are:

$$\frac{dN}{dt} = \nu - \frac{b}{n-1}N \tag{3.13}$$

$$\frac{\partial c}{\partial t} = D\frac{1}{r^2}\frac{\partial}{\partial r}\left(r^2\frac{\partial c}{\partial r}\right) - gc + bm - 2\nu + \beta \tag{3.14}$$

$$\frac{\partial m}{\partial t} = +gc - bm + 2\nu \tag{3.15}$$

where N (m^{-3}) is the number density of intra-granular bubbles, n is the number of gas atoms per bubble, c and m (m^{-3}) are the intra-granular gas concentration in the matrix and in the bubbles,

respectively, t (s) the time, D (m^2s^{-1}) the single-atom gas diffusion coefficient, r (m) the radial coordinate in the spherical grain, β ($m^{-3}s^{-1}$) the gas generation rate, g (s^{-1}) the trapping rate, b (s^{-1}) the re-solution rate. The coefficient 2 of the nucleation rate ν (atm $m^{-3}s^{-1}$), represents the fact that bubbles are nucleated as dimers.

The nucleation rate is calculated as:

$$\nu = 8\pi D R_{sg} f_n c^2 \tag{3.16}$$

where R_{sg} (m) is the radius of a single fission gas atom and f_n is the nucleation factor (/), equal to 10^{-6} (e.g., [16]). This system of equations is solved with an advanced version of the PolyPole algorithm [17].

Intra-granular bubble growth is treated using a modified [18] model. The mechanical equilibrium of an intra-granular bubble, assumed to be spherical, is governed by the Young-Laplace equation

$$p_{eq} = \frac{2\gamma}{R_b} - \sigma_h \tag{3.17}$$

where p_{eq} (Pa) is the equilibrium pressure, γ (J m^{-2}) is the U_3Si_2 gas surface energy and σ_h (Pa) is the hydrostatic stress. In general, the bubbles are in a non-equilibrium state and tend to the equilibrium condition absorbing or emitting vacancies. The vacancy absorption/emission rate can be calculated starting from the approach in [18] as

$$\frac{dn_{iv}}{dt} = \frac{2\pi D_{ig}^{v} \rho}{kT\zeta}(p - p_{eq}) \tag{3.18}$$

with n_{iv} (-) the number of vacancies per intra-granular bubble, D_{ig}^{v} (m^2 s^{-1}) the intra-granular vacancy diffusion coefficient, ρ (m) is the radius of the equivalent Wigner-Seitz cell surrounding a bubble and influenced by the vacancy absorption/emission, k (J K^{-1}) is the Boltzmann constant, T (K) is the local temperature, and ζ (-) is an dimensionless factor, which is calculated as [19]

$$\zeta = \frac{10\psi(1+\psi^3)}{-\psi^6 + 5\psi^2 - 9\psi + 5} \tag{3.19}$$

where $\psi = \dfrac{R_b}{\rho}$ is the ratio between the bubble and the cell radii. The approach presented here

differs from the original proposed in [18] because it involves a 3D representation of the absorption/emission phenomena, rather than a 2D description, which better suits the absorption/emission of vacancies at grain boundaries. For the diffusion coefficients, D and Dv_{ig}, and the re-solution rate, b, we use values for U_3Si_2 from the atomistic work of [20] and [15], respectively.

The pressure of the bubble is expressed as, considering a van der Waals gas,

$$p = \frac{kT}{\Omega - \eta\omega}\eta \tag{3.20}$$

where Ω (m^3) is the vacancy volume, η (-) is the ratio between $\bar{n}$ and n_{iv}, and ω (m^3) is the van der Waals atomic volume for xenon.

The volume of intra-granular bubbles is calculated as

$$V_b = n_{iv}\Omega \tag{3.21}$$

such that the radius is evaluated considering spherical bubbles

$$R_b = \sqrt[3]{\frac{3V_b}{4\pi}} \tag{3.22}$$

The intra-granular swelling is calculated as the average volume of the bubble with respect to the bubble number density.

The formation of the high burnup structure is not currently represented in the model, due to the lack of data on this phenomenon in U_3Si_2.

3.2.4.2 Grain-face gas behavior

The numerical solution of Eqs. 3.14 allows estimating the arrival rate of gas at the grain faces, providing the source term for the grain-face gas behavior module. This computes both the fission gas swelling and release through a direct description of the grain-face bubble development, including bubble growth and coalescence (which are reflected in fuel swelling), and the eventual inter-connection (leading to thermal fission gas release).

These conceptual steps and the related equations are identical to those applied in the existing UO_2 model in BISON. However, the material parameters are specific to the U_3Si_2 model. Nevertheless, in this model an initial concentration of grain-face bubbles equal to $2 \cdot 10^{12}$ is employed. The value is one order of magnitude lower than the one employed in UO_2, reflecting the lower bubble density noticeable in uranium silicide from the available experimental data [13].

The fractional volume grain-face fission gas swelling is given by

$$\left(\frac{\Delta V}{V}\right) = \frac{1}{2}\frac{N_{gf}}{(1/3)r_{gr}}\left(\frac{4}{3}\pi\varphi(\Theta)R_{gf}^3\right) \tag{3.23}$$

where N_{gf} is the number density of grain-face bubbles per unit surface, r_{gr} the grain radius, Θ the bubble semi-dihedral angle, $\varphi(\Theta)$ the geometric factor relating the volume of a lenticular-shape bubble to that of a sphere, which is $1 - 1.5\cos(\Theta) + 0.5\cos^3(\Theta)$, and R_{gf} the bubble radius of curvature. The factor 1/2 is introduced in Eq. 3.23 because a grain-face bubble is shared by two neighboring grains.

Bubble growth is calculated with the model of Speight and Beere [18], to describe the growth (or shrinkage) of grain-face bubbles as proceeding by absorption (or emission) of vacancies in grain boundaries, induced by the difference between the pressure of the gas in the bubble, p (Pa), and the mechanical equilibrium pressure, p_{eq} (Pa).

The approach is conceptually analogous to that applied for the growth and shrinkage of intra-granular bubbles. The diffusion coefficient of vacancies at grain boundaries is estimated by multiplying the intra-granular one by a factor of 10^7.

This approach computes the bubble growth rate from the rate of inflow of gas atoms and the rate of absorption (emission) of vacancies at the bubble. The combined effects of gas atom inflow and vacancy absorption (emission) are interactive, since the addition of fission gas atoms gives rise to a change in the bubble pressure, which affects the propensity of the bubble to absorb (or emit) vacancies. Given the volume, V_{gf}, of a lenticular bubble of circular projection, the bubble radius of curvature is calculated as

$$R_{gf} = \left(\frac{3V_{gf}}{4\pi\varphi(\Theta)}\right)^{\frac{1}{3}} \tag{3.24}$$

The process of grain-face bubble coalescence, which leads to a progressive decrease of the bubble number density throughout irradiation, is described with a model based on [21, 22]. According to this model, the rate of loss of bubbles by coalescence is given by

$$\frac{dN_{gf}}{dt} = -\frac{6N_{gf}^2}{3+4N_{gf}A_{gf}}\frac{dA_{gf}}{dt} \tag{3.25}$$

where N_{gf} and A_{gf} represent the number density and projected area of grain-face bubbles, respectively.

The release of fission gas to the fuel rod free volume after the inter-connection of grain-face bubbles and the consequent formation of pathways for gas venting to the fuel exterior (thermal release) is based on the principle of grain face saturation. More specifically, a saturation coverage concept is adopted that assumes once the fractional coverage, F, attains a saturation value, F_{sat}, the bubble number density and projected area obey the saturation coverage condition

$$F = N_{gf}A_{gf} = F_{sat} \tag{3.26}$$

where N_{gf} is the bubble number density and $A_{gf} = \pi\left(\sin\left(\Theta\right)\right)^2 R_{gf}^2$ is the bubble projected area on the grain face. In absence of experimental data on the maximum grain-face bubble coverage in U_3Si_2, the theoretical value $Fsat = \pi/4$ is used.

Eq. (3.26) implies that, after attainment of the saturation coverage, a fraction of the gas on the grain faces is released to the fuel exterior and thereby compensates for continuing bubble growth.

3.3 Thermal and Irradiation Creep

A preliminary model for thermal and irradiation creep of U_3Si_2 fuel based upon the work of Metzger [23] has been incorporated into BISON. Initial simulations have indicated that above a homologous temperature of 0.75 T_{melt} and a von Mises to shear modulus ratio greater than 10^{-5} unrealistically high creep rates are observed. Discussions with Metzger and other researchers at the University of South Carolina have indicated that additional work is currently being conducted to investigate and improve the model. Therefore, in the simulations presented in this work U_3Si_2 is treated as an elastic material. It is noted that for improved comparisons between U_3Si_2 and UO_2 fuel performance a thermal and irradiation creep model for U_3Si_2 should be used as it may offset some of the gaseous swelling that occurs. However, due to the only available model in the literature currently undergoing revision, it was deemed appropriate to treat the U_3Si_2 fuel as elastic.

4 Separate Effects Simulations

Separate effects tests examine the effects of individual material models on fuel performance parameters (e.g., temperatures, stresses, strains) of interest with minimal influence of other models. Separate effects tests can be used as a method of verification to ensure sure that the solution obtained matches what would be calculated analytically. In this Chapter, separate effects tests for thermal conductivity, volumetric swelling, and fission gas release are included with comparisons to results obtained using the corresponding UO_2 models in BISON. The details of the UO_2 models available in BISON are provided in the BISON theory manual [24].

4.1 Thermal Conductivity

One of the noted advantages of U_3Si_2 over UO_2 is the improved thermal conductivity. When this claim was initially made there was only data on unirradiated fuel thermal conductivity. With the development a thermal conductivity degradation model using the multiscale approach, comparisons of the thermal conductivity of U_3Si_2 and UO_2 including degradation (burnup) effects can be completed. For completeness both unirradiated and degraded thermal conductivity comparisons are given here. For simplicity the finite element domain analyzed is a 1 mm x 1mm x 1mm cube. In the unirradiated case the correlation suggested by White et al. [7] is used for U_3Si_2, whereas in the degraded case the model by Miao et al. [8] is used. For both cases the NFIR [25] model is used for UO_2. The temperature of the block is varied from 300 K to 1500 K over 100 seconds in the unirradiated case. In the degraded case the temperature variation is reduced to a maximum of 1100 K in order not to exceed the range of applicability of the degradation model for U_3Si_2. In addition to the temperature variation, different constant burnups of 0, 0.03 and 0.06 FIMA are applied to introduce burnup effects in the degraded case. No temperature gradient effects are included as the temperature is maintained constant throughout the sample. The porosity for all cases is 5% which represents a 95% theoretical density fuel.

The results for the unirradiated and degraded cases are illustrated in Figures 4.1a and 4.1b respectively.

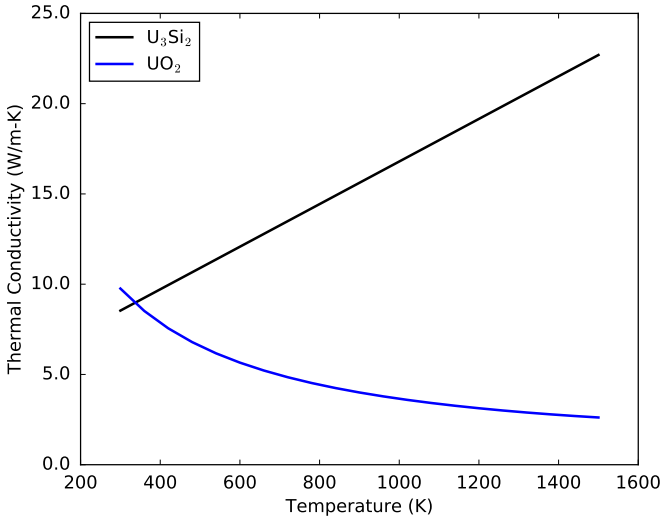

(a)

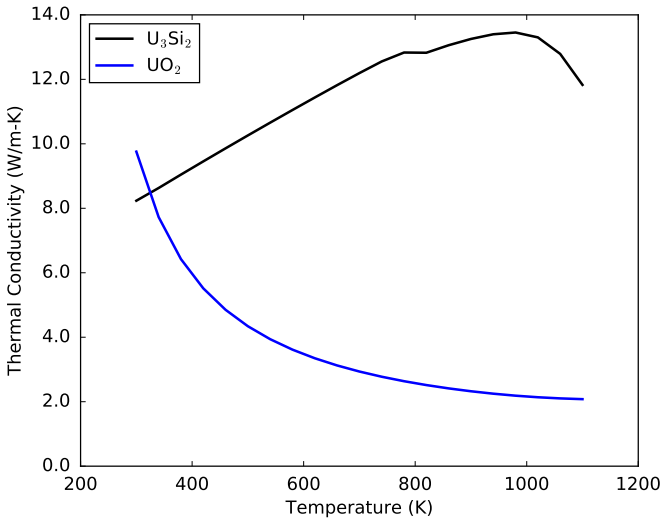

(b)

Figure 4.1: Temperature dependence of thermal conductivity for both (a) unirradiated and (b) degraded cases.

4.2 Volumetric Swelling

A potential issue with U_3Si_2 is the significant swelling that can occur at high burnups as observed by Finlay [11]. However, these observations were on dispersion fuel from research reactors. Therefore, here we compare the swelling predictions of the three models for U_3Si_2 described earlier in this report to the model for UO_2. For ease of understanding, the solid swelling and

gaseous swelling components are analyzed separately. In these analyses a 2D-RZ axisymmetric simulation of a single fuel pellet is used containing 11 finite elements in the radial direction and 5 axially. The pellets are solid (not annular) and both have an outer diameter of 9 mm. For the solid swelling investigation, the burnup is constant throughout the pellet and varies from 0 to 0.06 FIMA over 1e7 s. For gaseous swelling two cases are analyzed. In these cases in addition to the burnup variation, the temperature is held constant at 800 K and 1100 K with an initial grain radius of 10μm. For the UO_2 model and U_3Si_2 coupled fission gas release model, fission rate is required. A constant fission rate of 2e19 fissions/s is assumed. It should be recalled that the Argonne model is restricted to temperatures up to 1190 K, whereas the other two models are able to go to higher temperatures.

The solid swelling components are shown in Figure 4.2a. Recall that for U_3Si_2, regardless of the gaseous swelling model the solid swelling component correlation is the same. The differences appear in the gaseous swelling component. Thus only two curves are present in the figure, one representing UO_2 and one for U_3Si_2. The gaseous swelling component is shown in Figures 4.2b and Figures 4.2c with three lines for U_3Si_2 representing the empirical, Argonne, and coupled fission gas release (FGR) models.

The results indicate that UO_2 experiences more swelling due to solid fission products as seen by the larger slope of the lines in Figure 4.2a. For both the low temperature and high temperature cases it is observed that regardless of the model used U_3Si_2 experiences significantly larger gaseous swelling compared to UO_2. At high temperatures the gaseous swelling becomes extremely large in U_3Si_2 and is of significant concern for integral rod cases when stresses in the cladding are of significant importance in determining failure.

4.3 Fission Gas Release

The fission gas behavior within the fuel is of utmost importance as it degrades the thermal conductivity and the ability for heat to be removed in addition to increasing the internal rod pressure if the gases are released to the plenum. Overpressure of the rod due to fission gas release could lead to cladding failure under postulated accident conditions. In this study, two cases are presented for a a single fuel pellet with outer diameter of 9 mm. In one case the pellet is subjected to a constant fission rate 2e19 fissions/s and a constant temperature of 800 K for 1e7 seconds. In the second the temperature is increased to 1400 K. The increase in temperature between the two tests is to investigate the significant temperature dependence of fission gas release due to the larger diffusion coefficients of the fission gases at higher temperatures. The results of the two cases are show in Figures 4.3a and 4.3b, respectively.

The results indicate that no fission gas is released in both U_3Si_2 and UO_2 in the low temperature case and significantly higher fission gas is released from U_3Si_2 at high temperatures. It should be noted that during normal operation the centerline temperature is approximately 400 K less in

U_3Si_2 fueled rods compared to UO_2 rods [26]. Therefore, under integral rod conditions because of the increased thermal conductivity in U_3Si_2 resulting in lower operating temperatures, the fission gas released from U_3Si_2 is likely lower than from UO_2.

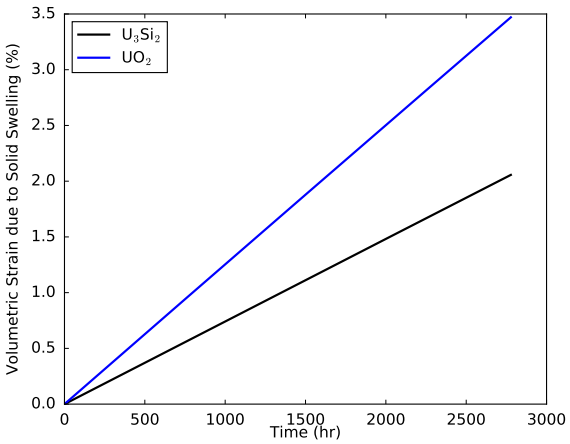

(a)

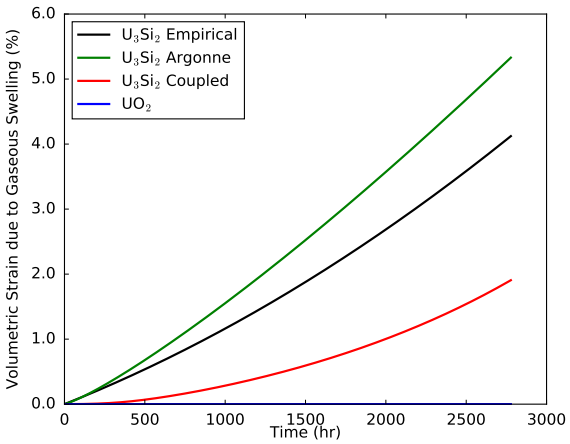

(b)

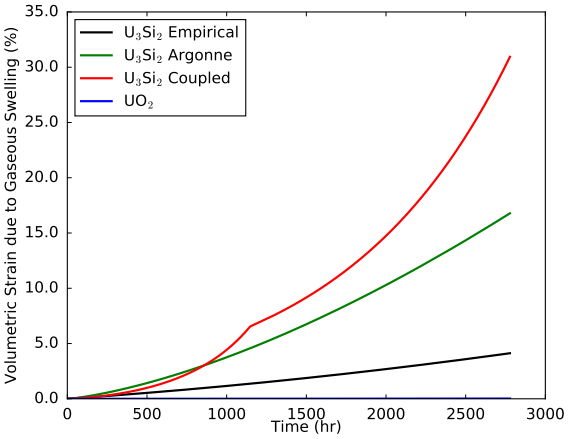

(c)

Figure 4.2: Volumetric strains due to swelling from (a) solid fission products (b) gaseous fission products at 800 K and (c) gaseous fission products at 1100 K.

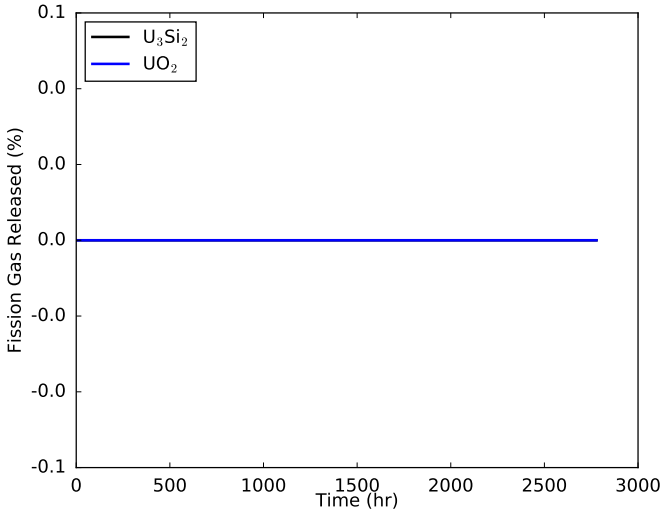

(a)

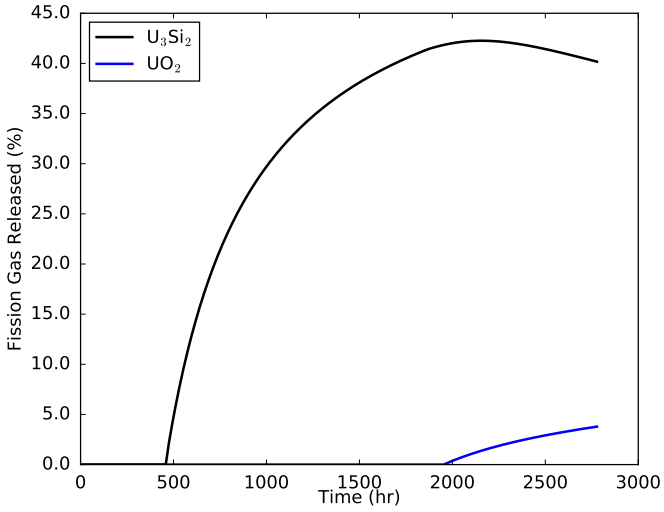

(b)

Figure 4.3: Fission gas released from U_3Si_2 and UO_2 as a function of time at (a) 800 K and (b) 1400 K.

5 Conclusions

The material and behavior models for U_3Si_2 fuel available in the BISON fuel performance code have been presented. Separate effects test comparisons between U_3Si_2 and the conventional fuel UO_2 were completed for thermal conductivity, volumetric swelling and fission gas release. It was observed that U_3Si_2 has larger thermal conductivity values compared to UO_2 even when taking into account thermal conductivity degradation. The contribution to total volumetric swelling from solid fission products is larger in UO_2 whereas the contribution from gaseous fission products is larger in U_3Si_2. At higher temperatures the gaseous fission product strain component becomes extremely large in U_3Si_2 and is an area for further investigation under integral conditions. At low temperatures neither U_3Si_2 or UO_2 experience any fission gas release. However, at higher temperature the fission gas model predicts a large portion of the fission gases are released from U_3Si_2.

6 Future Work

Comparisons between U_3Si_2 and UO_2 cladded rods for integral rod(let) simulations under light water reactor conditions is currently being completed. Integral simulations are different than separate effects in that all of the material models are included and the interdependencies are accounted for in the determination of the fuel performance parameters (i.e., fuel temperature, cladding stresses and strains, rod internal pressure, fission gas release). These comparisons will be for normal operating, loss of coolant accident, reactivity insertion accidents, and station black out conditions. Sensitivity analyses are also underway on select modeling parameters to highlight the importance of having uncertainty on parameters for which limited experimental data is available. The desire is to have these analyses help guide experimentalists in the future. The results will be presented in the end of HIP report due September 30, 2017.

7 Acknowledgements

Funding for this work is from the DOE Nuclear Energy Advanced Modeling and Simulation program through the Accident Tolerant Fuel High Impact Problem. The submitted manuscript has been authored by a contractor of the U.S. Government under Contract DE-AC07-05ID14517. Accordingly, the U.S. Government retains a non-exclusive, royalty free license to publish or reproduce the published form of this contribution, or allow others to do so, for U.S. Government purposes.

Bibliography

[1] S. Bragg-Sitton, B. Merrill, M. Teague, L. Ott, K. Rob, M. Farmer, M. Billone, R. Montgomery, C. Stanek, M. Todosow, and N. Brown. Advanced fuels campaign light water reactor accident tolerant fuel performance metrics. Technical Report INL/EXT-13-29957, Idaho National Laboratory, 2014.

[2] R. L. Williamson, J. D. Hales, S. R. Novascone, M. R. Tonks, D. R. Gaston, C. J. Permann, D. Andrs, and R. C. Martineau. Multidimensional multiphysics simulation of nuclear fuel behavior. *Journal of Nuclear Materials*, 423:149–163, 2012.

[3] J. D. Hales, S. R. Novascone, B. W. Spencer, R. L. Williamson, G. Pastore, and D. M. Perez. Verification of the BISON fuel performance code. *Annals of Nuclear Energy*, 71:81–90, 2014.

[4] R.L. Williamson, K.A. Gamble, D.M. Perez, S.R. Novascone, G. Pastore, R.J. Gardner, J.D. Hales, W. Liu, and A. Mai. Validating the BISON fuel performance code to integral LWR experiments. *Nuclear Engineering and Design*, 301:232 – 244, 2016.

[5] Nuclear energy advanced modeling and simulation (NEAMS) accident tolerant fuels high impact problem: Coordinate multiscale U_3Si_2 modeling. Technical Report INL/EXT-17-42828, Idaho National Laboratory, 2017.

[6] K. E. Metzger, T. W. Knight, and R. L. Williamson. Model of U_3Si_2 fuel system using BISON fuel code. In *Proceedings of the International Congress on Advances in Nuclear Power Plants - ICAPP 2014*, Charlotte, NC, April 6–9 2014.

[7] J. T. White, A. T. Nelson, J. T. Dunwoody, D. J. Safarik, and K. J. McClellan. Corrigendum to Thermophysical Properties of U_3Si_2 to 1777 K. *Journal of Nuclear Materials*, 484:386–387, 2017.

[8] Y. Miao, K. A. Gamble, D. Andersson, B. Ye, Z. Mei, G. Hofman, and A. M. Yacout. Gaseous swelling of U_3Si_2 during steady-state lwr operation: A rate theory investigation. *Nuclear Engineering and Design*, 322:336–344, 2017.

[9] J. T. White, A. T. Nelson, J. T. Dunwoody, D. D. Byler, D. J. Safarik, and K. J. McClellan. Thermophysical properties of U_3Si_2 to 1773K. *Journal of Nuclear Materials*, 464:275–280, 2015.

[10] Y. Rashid, R. Dunham, and R. Montgomery. Fuel analysis and licensing code: FALCON MOD01. Technical Report EPRI 1011308, Electric Power Research Institute, December 2004.

[11] J.L Snelgrove M. R. Finlay, G. L. Hofman. Irradiation behaviour of uranium silicide compounds. *Journal of Nuclear Materials*, 325:118–128, 2004.

[12] G. L. Hofman and W. S. Ryu. Detailed Analysis of Uranium Silicide Dispersion Fuel Swelling. Technical Report CONF-8909141–10, Argonne National Laboratory, 1989.

[13] H. Shimizu. The properties and irradiation behavior of U_3Si_2. Technical Report NAA-SR-10621, Atomics International, 1965.

[14] D. R. Olander and D. Wongsawaeng. Re-solution of fission gas – A review: Part I. Intragranular bubbles. *Journal of Nuclear Materials*, 354:94–109, 2006.

[15] C. Matthews, D.A. Andersson, and C. Unal. Radiation re-solution calculation in uranium-silicide fuels. Technical report, Los Alamos National Laboratory, 2016.

[16] M. S. Veshchunov. On the theory of fission gas bubble evolution in irradiated UO_2 fuel. *Journal of Nuclear Materials*, 277:67–81, 2000.

[17] D. Pizzocri, C. Rabiti, L. Luzzi, T. Barani, P. Van Uffelen, and G. Pastore. PolyPole-1: An accurate numeical algorithm for intra-granular fission gas release. *Journal of Nuclear Materials*, 478:333–342, 2016.

[18] M.V. Speight and W. Beere. Vacancy potential and void growth on grain boundaries. *Metal Science*, 9:190–191, 1975.

[19] D. Pizzocri, F. Cappia, V. V. Rondinella, and P. Van Uffelen. Preliminary model for the pore growth in the HBS. Technical report, JRC103064, European Commission, Directorate for Nuclear Safety and Security, JRC-Karlsruhe, 2016.

[20] D.A. Andersson. Density functional theory calculations of the defect and fission gas properties in U-Si fuels. Technical report, Los Alamos National Laboratory, 2017.

[21] G. Pastore, L. Luzzi, V. Di Marcello, and P. Van Uffelen. Physics-based modelling of fission gas swelling and release in UO_2 applied to integral fuel rod analysis. *Nuclear Engineering and Design*, 256:75–86, 2013.

[22] R.J. White. The development of grain-face porosity in irradiated oxide fuel. *Journal of Nuclear Materials*, 325:61–77, 2004.

[23] K. E. Metzger. *Analysis of Pellet Cladding Interaction and Creep of U_3Si_2 Fuel for Use in Light Water Reactors*. PhD thesis, University of South Carolina, 2016. Retrieved from http://scholarcommons.sc.edu/etd/3811.

[24] J. D. Hales, R. L. Williamson, S. R. Novascone, G. Pastore, B. W. Spencer, D. S. Stafford, K. A. Gamble, D. M. Perez, R.J. Gardner, and W. Liu. BISON theory manual: The equations behind nuclear fuel analysis. Technical Report INL/EXT-13-29930, Rev.2, September 2015.

[25] A. Marion (NEI) letter dated June 13, 2006 to H. N. Berkow (USNRC/NRR). Safety Evaluation by the Office of Nuclear Reactor Regulation of Electric Power Research Institute (EPRI) Topical Report TR-1002865, "Topical Report on Reactivity Initiated Accidents: Bases for RIA Fuel rod Failures and Core Coolability Criteria". http://pbadupws.nrc.gov/docs/ML0616/ML061650107.pdf, 2006.

[26] Kyle A. Gamble and Jason D. Hales. Preliminary evaluation of FeCrAl cladding and U-Si fuel for accident tolerant fuel concepts. In *TopFuel 2015 Conference Proceedings*, Zurich, Switzerland, 13–17 September 2015.